High-resolution three-dimensional computed tomography for materials from industrial field

Three-dimensional synchrotron-radiation-based imaging has been defined as one of the new global technologies for the visualization of internal features of biological, chemical and material substances. With the recent developments in X-ray detectors and personal computers, three-dimensional computed tomography (3D CT) has generated interesting images with no additional data treatments like Fourier transformation, this fact being very attractive even for non-experts of X-rays.

Hyogo Prefectural contract beamlines, **BL08B2** and **BL24XU**, have provided opportunities for various users from industries to perform 3D CT experiments for fairly large samples (at BL08B2) and small samples (at BL24XU) to observe very local volumes.

CT systems utilizing highly brilliant undulator emission at BL24XU are available based on simple projection imaging with absorption and/or refraction contrast using a visible-ray-conversion-type X-ray imager. The X-ray energy is discretely selectable from 10 to 30 keV for every 5 keV using a silicon double-crystal monochromator. The field of view is limited by the incoming beam size of 2 mm (horizontal) by 1.5 mm (vertical). The typical X-ray intensity of 10 keV is about 1×10^{13} photons/s.

Two types of system are open for industrial users. One is for high-spatial-resolution CT combined with a YAG single-crystal scintillator. The spatial resolution of about 1 μm is possible with a typical measurement time of 1 h. The other system is for high-speed CT introducing a P46-type high-speed phosphor screen and a high-speed CMOS sensor. The acquisition time for single CT is 0.14 sec with the spatial resolution of 14 μm. This system can work with continuous sample rotation and image acquisition up to 2 gigabytes of data, so that 4D (3D + time) CT measurement to observe the dynamics of the internal structure is available.

The thermal change or solution reaction in a sample can be observed with this system. Figure 1 shows typical images obtained with both systems with 10 keV X-rays. Figure 1(a) shows volume-rendering images of a casting of carbon fibers of 7 μm diameter obtained by the high-spatial-resolution system. The image is reconstructed using 1200 projections with the effective pixel size of 0.95 μm. In the right figure (a magnified figure of the left), the local orientation of the fibers can be clearly seen. Figure 1(b) shows a rendering image and a sliced image of the solution with the bubbles of detergent in a glass capillary obtained by the high-speed system. The CT reconstruction is made using 361 projections with the acquisition time of 0.144 sec (2500 frames/sec). In this setting, continuous measurement of about 5000 images, corresponding to 14 CTs, is achievable.

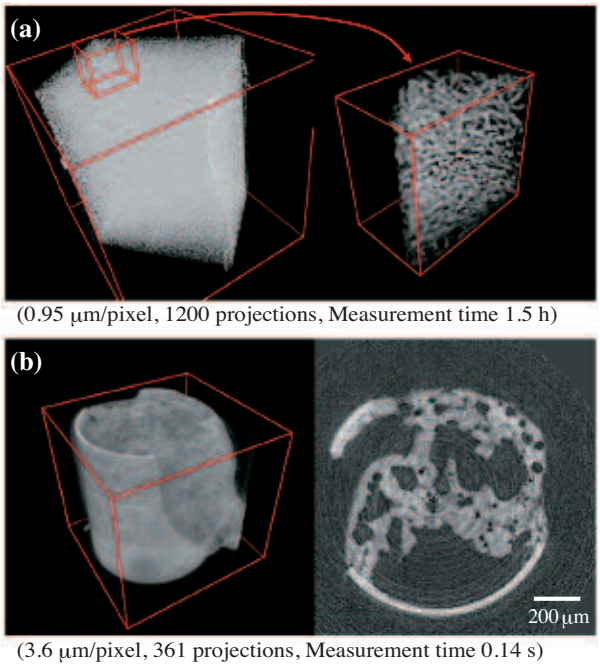

(0.95 μm/pixel, 1200 projections, Measurement time 1.5 h)

(3.6 μm/pixel, 361 projections, Measurement time 0.14 s)

Fig. 1. Typical CT images obtained at BL24XU. **(a)** Volume-rendering images (right: magnified image of the left image) of a casting of carbon fibers of 7 μm diameter obtained by the high-spatial-resolution system. **(b)** A volume-rendering image and a sliced image of a bubbling solution of detergent in a glass capillary obtained using the high-speed system.

Furthermore, other CT systems for ultrahigh resolution are under development using X-ray optical devices as scientific research at the University of Hyogo. A micro-interferometer system based on X-ray imaging microscopy for phase contrast CT with 200 nm resolution and a phase contrast scanning CT system using an X-ray focusing beam have been developed. Figure 2 shows typical images obtained

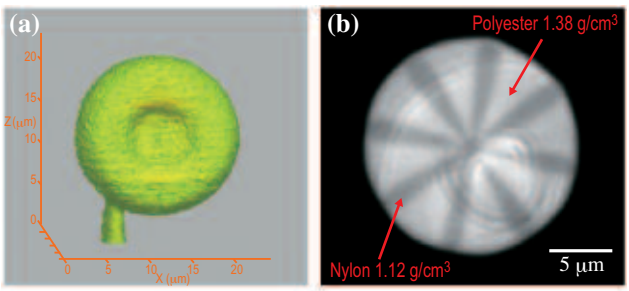

(33 nm/pixel, 180 projections) (200 nm/pixel, 300 projections)

Fig. 2. Typical CT images obtained by the ultrahigh-resolution system in BL24XU. **(a)** A volume-rendering image of a diatom obtained using the micro-interferometer. **(b)** A sliced image of a composite fiber of polystyrene and nylon obtained using the scanning system.

using both systems with 10 keV X-rays. A volume-rendering image of a diatom obtained using the micro-interferometer is shown in Fig. 2(a), and a sliced image of a composite fiber of polystyrene and nylon obtained using the scanning system with a focusing beam of 0.4 μm size is shown in Fig. 2(b).

In BL08B2, on the other hand, a new experimental station for a large-viewfield CT exploiting a characteristic in wide X-ray beams from a bending magnet light source has been constructed at 2010A. The monochromated X-ray beams with an energy ranging from 5 to 30 keV are selectable for the CT experiments. To achieve both the large viewfield and the high spatial resolution, a visible-ray-conversion type X-ray imager with a 4008×2672-element CCD camera is employed. Two types of scintillators, a cerium-doped lutetium oxyorthosilicate (LSO) single-crystal screen for a high-spatial-resolution CT and a P43-type powder phosphor screen for the large-viewfield CT, are available in this imager. The viewfield ranges from a few mm with the effective pixel size of sub-μm to 20 mm (horizontal) by 10 mm (vertical) with the effective pixel size of 5 μm. The CT measurement takes typically 0.5 – 2 h.

The large-viewfield CT system can be used to observe many industrial materials without any prior processes. Typical images obtained with this system are shown in Fig. 3. The observed samples are drug tablets of 5 – 10 mm size. The CT reconstructions are made using 1000 projections with the effective pixel size of 4.28 μm. Active substances, excipients and outer coating layer were clearly visible. The CT can provide crucial information about the tabletting formulations such as uniformity of the active substances and thickness of the coating layer.

We have carried out a CT experiment of a resin foam as an example for industrial use [1]. The resin foam exhibits excellent impact and shock absorption properties, and is utilized as a cushion materials, for instance, as a shoe sole. The CT observations of the resin foam under compressive deformation were carried out to interpret cell deformation behaviors in the resin foam, which is directly linked to the impact and shock absorption properties. Figure 4 shows the CT images of the resin foam before and after applying uniaxial compressive deformation. It is seen that the cells are collapsed with the increase in the compressive strain. The deformation behaviors of each cell can also be tracked out by the sequential measurements. To elucidate the deformation mechanism more in detail, further analysis combining the obtained CT data and a finite element method is now in progress.

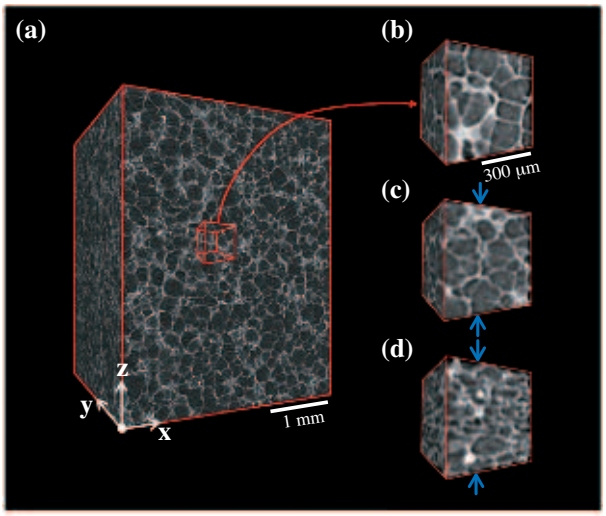

(4.28 μm/pixel, 1000 projections, Measurement time 1.2 h)

Fig. 4. Volume-rendering images of a resin foam. **(a)** Overview image of the sample before compression. Magnified images around the center of the sample **(b)** before and under the compressive strains of **(c)** 20% and **(d)** 40%. The sample was compressed parallel to the z-axis.

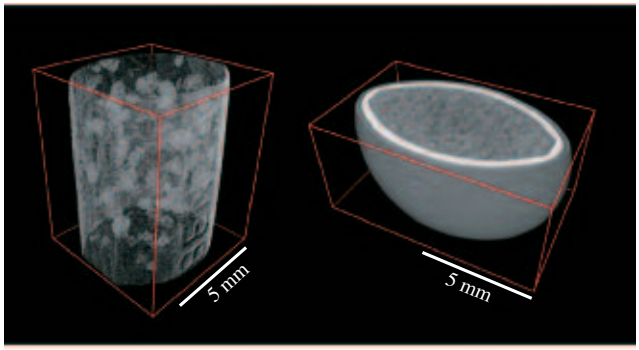

(4.28 μm/pixel, 1000 projections, Measurement time 1.2 h)

Fig. 3. Volume-rendering images of drug tablets.

Hidekazu Takano[a,*], Yoshimasa Urushihara[b] and Junji Matsui[b]

[a] Graduate School of Material Science, University of Hyogo
[b] Synchrotron Radiation Nanotechnology Lab., Hyogo Science and Technology Association

*E-mail: htakano@sci.u-hyogo.ac.jp

References

[1] J. Tateishi *et al.*: in preparation.